Journal of Alloys and Compounds 766 (2018) 104–111

Contents lists available at ScienceDirect

Journal of Alloys and Compounds

journal homepage: http://www.elsevier.com/locate/jalcom

Electronic properties of porous graphene and its hydrogen storage potentials

Ming Min Zhong [a, *], Hong Kuan Yuan [a], Cheng Huang [a], Guangzhao Wang [b, **]

[a] School of Physical Science and Technology, Southwest University, Chongqing 400715, China
[b] School of Electronic Information Engineering, Yangtze Normal University, Chongqing, 408100, China

ARTICLE INFO

Article history:
Received 4 April 2018
Received in revised form
11 June 2018
Accepted 26 June 2018
Available online 28 June 2018

Keywords:
Graphene nanomesh
BN nanomesh
Electronic structure
Two mechanisms
Hydrogen storage capacity

ABSTRACT

First principles calculation based on density functional theory has been applied to systematically study the electronic structure, especially band gap of recently synthesized periodic porous structure, graphene nanomesh, as well as its analogous system BN nanomesh. These porous structures possess various band gaps due to two parameters: neck length and width. The modulation of these parameters can be achieved through different etching templates in experiments. Two mechanisms, plane and nanoribbon, are proposed to understand the band gap variation with respect to neck length and width, qualitatively. We also examine electronic frontier states around Fermi level. Especially, armchair necked BN nanomesh has separated highest occupied and lowest unoccupied states in real space, which also makes it be reactive at different site. The hydrogen storage potentials based on transition metal atoms such as Sc trapped in anionic decorated pores are also been explored. No clustering problem is found and one Sc can adsorb four H_2 molecules with binding energy per H_2 of 0.13 eV.

1. Introduction

Graphene [1], single atomic layer of graphite, has attracted great attention of scientists due to its high mechanical property, thermoconductivity, Klein tunneling, and anomalous quantum Hall effect [2]. Besides, owing to Dirac point in its reciprocal space, electrons of graphene behave like mass-less electrons, hence electron mobility of graphene is rather high even at room temperature [3]. Since graphene can be viewed as a semi-metallic material with no band gap and cannot be applied directly in nano-electronic devices, it is desirable to open its band gap in feasible and controllable methods [4]. Current strategy of tuning the band gap of graphene can be classified into mainly three groups. The first one is to absorb single atoms (such as H and F) or small molecules on its surface [5–12]. Hydrogenated graphene has been first predicted [5] and then achieved experimentally [6] by exposing graphene in H plasma environment, which can convert sp^2 hybridized C atoms into sp^3 hybridization, and consequently opens the band gap. Theoretical studies show that different absorption atoms and topological absorptions can lead to different band gaps, which is, however, not easy to be achieved in experiment. The second strategy is to cut graphene sheet into 1D nanoribbon (GNR) or 0D quantum dot [13,14]. It is shown that the band gaps of armchair edged nanoribbons (AGNR) generally decrease with increasing the widths separately in 3p, 3p+1 and 3p+2 groups, while zigzag edged nanoribbons (ZGNR) have first increase and then decrease band gap variation with respect to their widths [14]. Although nanoribbons can be cut from graphene with the help of oxygen in experiment, the width should be less than 10 nm in order to achieve significant band gap and the driving current is not high [15]. The third one is to introduce some doped foreign atoms such as B and N [16–19]. For example, Ci et al. have successfully embedded BN sheet into graphene through the thermal catalytic chemical vapor deposition (CVD) method [17]. This can lead to various band gaps of graphene sheet according to different concentrations of BN and embedding patterns. Besides the above three methods, recently, based on block copolymer lithography technology, Bai et al. have synthesized novel uniform and periodic porous graphene (graphene antidot) in large extent [20]. They refer to it as graphene nanomesh (GNM) which can be viewed as *super-graphene*. The periodicity of pores and width of neck can be modulated in a feasible way. It is shown that this nanomesh can bear current of ~100 times than graphene nanoribbon, and also the on-off ratio can be tuned through the

* Corresponding author.
** Corresponding author.
E-mail addresses: zhongmm@swu.edu.cn (M.M. Zhong), wangyan6930@yznu.edu.cn (G. Wang).

https://doi.org/10.1016/j.jallcom.2018.06.323
0925-8388/

width of its neck [20]. Similar porous structures have also been synthesized [21–26]. But few theoretical works have been carried out to investigate the details of band gap modulation of GNM.

In this article, using first-principles calculations, we study the band gap and electronic properties of nanomesh. The band gap dependence on the chirality, length and width of GNM neck is systematically explored. Besides graphene, another 2D sp^2 hexagonal single atomic layer, BN sheet, has also been synthesized in experiments through a chemical-solution-derived method from single-crystalline hexagonal boron nitride [27]. Therefore, we also take analogous structures based on BN sheet, BN nanomesh (BNNM) into consideration. We demonstrate that the band gap and electronic structure of GNM and BNNM can be modulated through different etching patterns. At last, through oxygen decoration of the pores, we show that the pores can be traps of transition metals (TM) Sc, which was used as hydrogen storage material in pure organic structures such as C_{60} without clustering problem [28]. This motivates us to explore the potential application of GNM and BNNM in hydrogen storage.

2. Computational methods

All results are obtained using first-principles calculations based on density function theory (DFT). The generalized gradient approximation (GGA) with Perdew-Burke-Ernzerhost (PBE) form is employed for exchange-correlation functional [29]. The calculations have been implemented in Vienna *ab initio* simulation package (VASP) with periodic boundary condition and ultrasoft pseudopotential for each atom [30,31]. All of the C, B and N atoms are assumed to be sp^2 hybridized with dangling bonds saturated by H atoms. As shown in Fig. 1, we label armchair and zigzag necked GNMs by their neck chirality (A or Z), length (m) and width (n) in form of A(Z)-GNM (m, n). And for BNNM similar labels are applied. For example, structures in Fig. 1a and b are denoted as A-GNM (4, 3) and Z-GNM (6, 2), respectively. The same as Bai et al., we call the edge of NM as *neck*, and for convenience also refer to connecting point of necks as *node*. Vacuum space of 15 Å in *z* direction is used in order to avoid interactions between two neighboring images. Reciprocal space is represented by Monkhorst-Pack special *k* point scheme [32] with separation between two nearest *k* points less than 0.04 $Å^{-1}$, and for large unit cells, at least $3 \times 3 \times 1$ meshes are used. Geometric structural relaxations are based on conjugated gradient method. Convergence of total energy, Hellman-Feynman force, and energy cutoff are set to be 1×10^{-4} eV, 0.02 eV/Å and 400 eV, respectively. We also plot wave functions of each band near Fermi level at Γ point in DMol^3 software (PBE exchange correlation functional and DNP basis set) [33,34]. The accuracy of our calculation procedure has been tested in the previous work [35,36].

3. Results and discussion

3.1. Electronic structures of A-GNMs and A-BNNMs

First we study armchair necked GNM and BNNM. All the relaxed A-GNMs and A-BNNMs retain their planar structures without any buckles. For the A-GNMs, the bond lengths of C—C are calculated between 1.38 Å and 1.46 Å (Fig. 2a), which are in agreement with that in pure graphene sheet, namely, 1.42 Å. In more detail, the bond lengths of C—C linking two hexagonal C rings are lengthened to 1.46 Å; while the C—C bonds in the hexagonal C ring are slightly shortened compared with that of pure graphene. The C—H bond lengths are 1.08 Å, which are also in accordance with those in graphene nanoribbon. For the A-BNNMs, the B—N bond lengths are in the range of 1.41 Å ~1.46 Å, and elongation again happens on the bond linking two hexagonal BN rings (Fig. 2b). The relaxed B—H and N—H bond lengths are 1.20 Å and 1.02 Å, respectively, similar as in their free dimer states [37].

The electronic property calculations of A-GNM and A-BNNM show that all the structures are non-magnetic semiconductors. This non-magnetic property is also consistent with hexagonal graphene antidot [38] and Lieb's theorem [39], which can predict magnetic moment of bipartite structure by a simple counting rule. In Fig. 3 we plot the band structure, wave function at Γ point, and corresponding partial density of state (PDOS) of A-GNM (2, 3) and A-BNNM (2, 3). The valence band maximum (VBM) and conductance band minimum (CBM) are both located at K point in reciprocal space with band gap of 2.30 eV and 4.33 eV, respectively, indicating direct semiconducting nature. PDOS analysis shows that the band gap is contributed from *p* orbital. The band gap of GNM and BNNM can be understood based on mainly two mechanisms. The first one is called as *plane* mechanism, which compares porous structure with corresponding pure sheet. If the area of the pore is larger, the band gap will be far away from that of pure sheet. Specially speaking, larger pores of GNM can lead larger band gap, and for BNNM we find the band gap will decrease as pores become larger. This actually is a whole 2D effect consideration. On the other side, since the nanomesh can be viewed as framework of nanoribbon, we term the second one as *nanoribbon* mechanism. Longer neck has relatively small band gap because of larger hybridization. Generally speaking, for the longer and thinner the neck (large m and small n) nanomesh, the *nanoribbon* mechanism dominates, while for the shorter and wider the neck (small m and large n) nanomesh, the *plane* mechanism dominates. It should be emphasized that these two mechanisms are only qualitative consideration and the node of

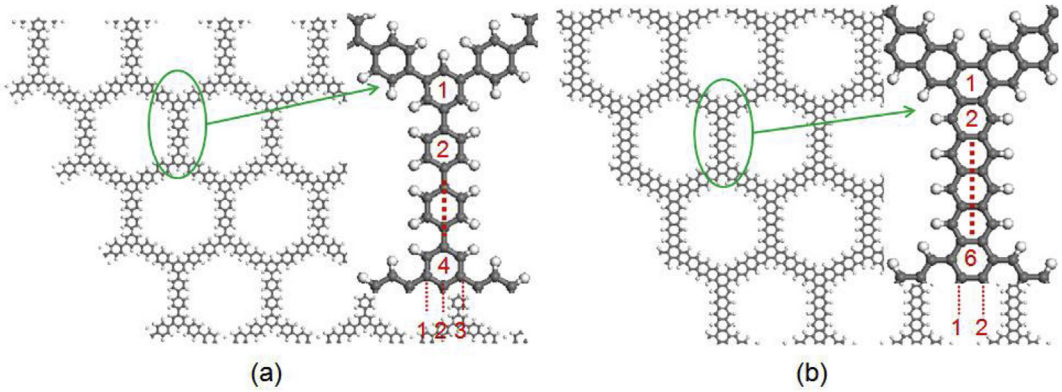

Fig. 1. Structure and symbol of (a) A-GNM (m, n) where m = 4, n = 3 and (b) Z-GNM (m, n) where m = 6, n = 2.